AAPS PharmSciTech, Vol. 15, No. 6, December 2014 (© 2014)
DOI: 10.1208/s12249-014-0182-z

Research Article

Theme: Advances in Formulation and Device Technologies for Pulmonary Drug Delivery
Guest Editors: Paul B. Myrdal and Steve W. Sein

High-Performing Dry Powder Inhalers of Paclitaxel DPPC/DPPG Lung Surfactant-Mimic Multifunctional Particles in Lung Cancer: Physicochemical Characterization, *In Vitro* Aerosol Dispersion, and Cellular Studies

Samantha A. Meenach,[1,2] Kimberly W. Anderson,[2,3] J. Zach Hilt,[2,3] Ronald C. McGarry,[4] and Heidi M. Mansour[5,6]

Received 29 April 2014; accepted 23 July 2014; published online 20 August 2014

Abstract. Inhalable lung surfactant-based carriers composed of synthetic phospholipids, dipalmitoylphosphatidylcholine (DPPC) and dipalmitoylphosphatidylglycerol (DPPG), along with paclitaxel (PTX), were designed and optimized as respirable dry powders using organic solution co-spray-drying particle engineering design. These materials can be used to deliver and treat a wide variety of pulmonary diseases with this current work focusing on lung cancer. In particular, this is the first time dry powder lung surfactant-based particles have been developed and characterized for this purpose. Comprehensive physicochemical characterization was carried out to analyze the particle morphology, surface structure, solid-state transitions, amorphous character, residual water content, and phospholipid bilayer structure. The particle chemical composition was confirmed using attenuated total reflectance-Fourier-transform infrared (ATR-FTIR) spectroscopy. PTX loading was high, as quantified using UV-VIS spectroscopy, and sustained PTX release was measured over weeks. *In vitro* cellular characterization on lung cancer cells demonstrated the enhanced chemotherapeutic cytotoxic activity of paclitaxel from co-spray-dried DPPC/DPPG (co-SD DPPC/DPPG) lung surfactant-based carrier particles and the cytotoxicity of the particles *via* pulmonary cell viability analysis, fluorescent microscopy imaging, and transepithelial electrical resistance (TEER) testing at air-interface conditions. *In vitro* aerosol performance using a Next Generation Impactor™ (NGI™) showed measurable powder deposition on all stages of the NGI and was relatively high on the lower stages (nanometer aerodynamic size). Aerosol dispersion analysis of these high-performing DPIs showed mass median diameters (MMADs) that ranged from 1.9 to 2.3 μm with excellent aerosol dispersion performance as exemplified by high values of emitted dose, fine particle fractions, and respirable fractions.

KEY WORDS: lung surfactant; NBD-PC fluorescent microscopy imaging; Next Generation Impactor (NGI); particle engineering design; pulmonary cell lines.

[1] Drug Development Division, Department of Pharmaceutical Sciences, College of Pharmacy, University of Kentucky, Lexington, Kentucky 40536, USA.
[2] Department of Chemical and Materials Engineering, College of Engineering, University of Kentucky, Lexington, Kentucky 40506, USA.
[3] Center of Membrane Sciences, University of Kentucky, Lexington, Kentucky, USA.
[4] Department of Radiation Medicine, College of Medicine, University of Kentucky, Lexington, Kentucky 40536, USA.
[5] Skaggs Pharmaceutical Sciences Center, College of Pharmacy, The University of Arizona, 1703 E. Mabel St, Tucson, Arizona 85721, USA.
[6] To whom correspondence should be addressed. (e-mail: mansour@pharmacy.arizona.edu)

INTRODUCTION

Lung cancer is the leading cause of cancer-related death in patients in the USA, and it is estimated that there will be 224,210 new cases diagnosed in 2014 leading to 163,660 deaths (1). While chemotherapy plays a significant role in the treatment of lung cancer in both the primary and supportive care of patients, it often leads to life-threatening side effects, especially in patients who are elderly or with late-stage disease. This work focuses on the direct delivery of dry powder particle aerosols containing the chemotherapeutic paclitaxel to the lung for the treatment of lung cancer. The lung is an attractive target for such drug delivery systems as direct delivery to the lung results in the avoidance of first-pass metabolism, a more rapid onset of therapeutic

action, and direct delivery to the site of treatment (2). Furthermore, while intravenous administration can provide high systemic drug concentrations for a short period of time, typically, a relatively low amount actually reaches the lung. A low lung-to-plasma ratio can potentially lead to treatment failure (3,4). Since the mass of the lung is typically 200 to 300 g (*e.g.* 0.35% of total body weight), the total amount of drug needed to adequately expose the entire tissue *via* inhalation therapy is small in comparison to what is necessary *via* the intravenous route (5). Several clinical studies have shown that inhalation of chemotherapeutic drugs can be equally or more effective than intravenous administration provided that the local lung concentration is high enough (6,7). Moreover, this type of treatment can result in improved drug tolerability allowing for higher-mass-tolerated doses to be achieved (3).

Dry powder inhalers (DPIs) offer many advantages including minimal patient hand-lung coordination, absence of propellant, portability, improved stability over liquid aerosols, and shorter inhalation treatment times (8,9). Another advantage of dry powder formulations is that they allow for the delivery of compounds that are poorly water soluble and difficult to deliver as inhaled aqueous solutions *via* pressurized metered-dose inhalers (pMDIs) or nebulization. Furthermore, they can be produced *via* spray-drying which offers a high-throughput method of solid-state particle engineering design and manufacture. Spray-drying is a versatile platform capable of microencapsulating a wide variety of compounds and is used often for pharmaceutical drugs. Dry powder formulations can benefit from particle engineering in that it can allow for the design of critical features into the systems including improved stability, improved powder dispersibility, controlled release, and/or increased drug permeability (10). Also, sustained release from a therapeutic aerosol may prolong the residence time of an administered drug in the airways or alveolar region, which could increase patient compliance by reducing dosing frequency (11). Particle engineering can involve the controlled production of particles of optimized size, morphology, and structure by formulation techniques, post-processing, optimization of milling processes, and novel formulation approaches (12). In particular, spray-drying offers many advantages in the production of particles for DPIs including increasing the stability of phospholipids by rendering them into the solid state (13). By reducing the amount of residual water present in the solid-state particles by organic solution spray-drying, physical and chemical stability can be improved. In addition, aerosol dispersion can be enhanced for particles delivered *via* DPIs by reducing the capillary forces between particles.

Paclitaxel (PTX) is a clinically well-established and highly effective anticancer agent for the treatment of many carcinomas (14). Clinically, PTX is a first-line drug used in the treatment of non-small cell lung cancer. It has been reported that PTX encapsulated in poly(ethylene glycol) distearoylphosphatidylethanolamine (DSPE-PEG) micelles exhibited sustained release and high concentration in the lungs of rats following intratracheal liquid aerosol administration using the PennCentury MicroSprayer® in comparison to intravenously delivered PTX (15). PTX was also loaded into alginate microparticles formulated *via* an emulsion technique which resulted in particles with an aerodynamic diameter of 5.9 μm and a fine particle fraction (FPF) of 14% (16).

In this study, the phospholipids, dipalmitoylphosphatidylcholine (DPPC) and dipalmitoylphosphatidylglycerol (DPPG), were rationally selected as nanocarriers in a lung surfactant-mimic molar ratio of DPPC:DPPG 75:25. They are the primary phospholipid component naturally present in the lung and are essential to proper lung surfactant function (17,18). The resulting particles that are converted into powders tend to form their thermodynamically stable multilamellar state (13), and unlike other inhaled particles, the fate of these components is similar to that of native lipids (19).

The described particles were analyzed for their effect on lung epithelial cells by measuring the transepithelial electrical resistance (TEER) of these cells. Since TEER evaluates the integrity of a cell monolayer, TEER reduction has been used as an indication of adverse effects of model toxicants and inhaled delivery vehicles and these results correspond well with standard toxicological tests (20). In this study, the bronchial lung cancer cell line, Calu-3, was used as a representative model of the airway epithelial barrier. The cells were grown in air-interface culture (AIC) conditions in Transwells where media were available on the basolateral side of the wells, but the lack of media on the apical side resulted in cells grown in contact with air. When grown using AIC, the lung cell layers resemble the native epithelium to a greater extent than cells grown in media in which the cells display enhanced ciliogenesis, increased mucus secretion, and more physiological TEER values (21).

Overall, the objective of this study was to design solid-state particles for inhalation containing PTX in DPPC/DPPG lung surfactant-mimic carriers using organic solution co-spray-drying in closed mode for targeted pulmonary delivery as microparticulate/nanoparticulate dry powder inhalation aerosols and test efficacy on model lung cancer cell lines. To the authors' knowledge, this systematic study is the first to report on the solid-state particle engineered design and comprehensive characterization of PTX encapsulated in lung surfactant-based carriers.

MATERIALS AND METHODS

Materials

Synthetic DPPC (molecular weight 734.039 g mol^{-1}, >99% purity) and DPPG (molecular weight 744.952 g mol^{-1}, >99% purity) were obtained from Avanti Polar Lipids (Alabaster, AL, USA). Paclitaxel was obtained from LC Laboratories (Woburn, MA, USA; 99.5% purity; $C_{47}H_{51}NO_{14}{\cdot}H_2O$). Methanol (HPLC grade, ACS certified) and chloroform (HPLC grade, ACS certified) were obtained from Fisher Scientific (Pittsburg, PA, USA). HYDRANAL®-Coulomat AD, Tween® 80, Cremophor® EL, and glycine were from Sigma-Aldrich (St. Louis, MO, USA). Ultra-high purity (UHP) dry nitrogen gas was from Scott-Gross (Lexington, KY, USA). All materials were used as received and stored at −23°C.

Advanced Spray-Drying from Organic Solution

Advanced co-spray-drying (co-SD) of paclitaxel-loaded lung surfactant-mimic particles was performed using a B-290 Büchi Mini Spray Dryer coupled with a B-295 Inert Loop and

high-performance cyclone (Büchi Labortechnik AG, Switzerland) in closed mode using UHP dry nitrogen as the atomizing gas. The stainless steel nozzle diameter was 0.7 mm, and the co-SD particles were separated from the drying gas *via* dry nitrogen in the high-performance cyclone and collected in a small glass sample collector. The feed solutions were prepared by co-dissolving DPPC and DPPG in the lung surfactant-mimic molar ratio of DPPC:DPPG 75:25 with different amounts of PTX including 0%, 25%, 50%, and 75% PTX on a molar basis to total DPPC and DPPG in methanol to form dilute total concentration feed solutions of 0.1% *w/v* 100% PTX spray-dried under these conditions, as recently reported by the authors (22). Based on our previous work (22,23), the following spray-drying conditions were used: atomization gas flow rate of 600 l h^{-1}, aspiration rate of 35 m^3 h^{-1}, inlet temperature of 150°C (which represents the primary drying step), and three different pump rates which represent "low P", "med P", and "high P" pump rates which correspond to 3, 15, and 30 ml min^{-1}, respectively. Particles with DPPC and DPPG only (hereby abbreviated 0PTX:100DPPC/DPPG) were SD at low P, med P, and high P, whereas particles containing PTX, DPPC, and DPPG (25PTX:75DPPC/DPPG, 50PTX:50DPPC/DPPG, and 75PTX:25DPPC/DPPG) were SD at high P only. All SD powders were stored in glass vials sealed with parafilm in desiccators over the indicated Drierite™ desiccant at −23°C under ambient pressure.

Scanning Electron Microscopy for Morphology and Shape Analysis

The shape and surface morphology of particles were evaluated by scanning electron microscopy (SEM), using a Hitachi S-4300 microscope (Tokyo, Japan), using similar conditions that we have previously reported (22,23). Samples were placed on double-sided adhesive carbon tabs adhered to aluminum stubs (Ted Pella, Inc., Redding, CA, USA) which were coated with a gold/palladium alloy thin film using an Emscope SC400 sputter coating system at 20 μA for 1 min under argon gas. The electron beam with an accelerating voltage of 5 kV was used at a working distance of 12.5–13.4 mm. Images were captured at several magnifications.

Particle Sizing and Size Distribution

The mean size, standard deviation, and size range of the particles were determined digitally using SigmaScan™ 5.0 software (Systat, San Jose, CA, USA), using similar conditions that we have previously reported (22,23). Representative micrographs for each particle sample at ×5,000 magnification were analyzed by measuring the diameter of at least 100 particles per image.

Karl Fischer Coulometric Titration

The water content of all particle powders was chemically quantified by Karl Fischer (KF) coulometric titration, using similar conditions reported by the authors (22,23). The measurements were performed with a 737 KF Coulometer coupled with 703 Ti Stand (Metrohm Ltd., Antwerp, Belgium). Approximately 5 mg of powder was dissolved in a known volume of chloroform. The sample solution was injected into the reaction cell that contained HYDRANAL® KF reagent, and the water content was then calculated from the resulting reading.

Differential Scanning Calorimetry

Thermal analysis and phase transition measurements were carried out using a TA Q200 differential scanning calorimetry (DSC) system (TA Instruments, New Castle, DE, USA) equipped with T-Zero® technology and an automated computer-controlled RSC-90 cooling accessory, using similar conditions reported by the authors (22,23). A mass of 1–3 mg of powder was weighed into hermetic anodized aluminum T-Zero® DSC pans and were hermetically sealed with the T-Zero® hermetic sealer (TA Instruments, New Castle, DE, USA). An empty hermetically sealed aluminum pan was used as the reference pan. UHP dry nitrogen gas was used as the purging gas at 50 ml min^{-1}. The heating range was 0–250°C at a heating scan rate of 5.00°C min^{-1}. All experiments were done in triplicate (n=3).

X-ray Powder Diffraction

X-ray powder diffraction (XRPD) patterns of powder samples were measured by a Rigaku Multiflex X-ray diffractometer (The Woodlands, TX, USA) with a slit-detector Cu Kα radiation source (40 kV, 44 mA, and λ=1.5406 Å), using similar conditions reported by the authors (22,23). The scan range was 5–50° (2θ) with a scan rate of 2° min^{-1} at ambient temperature. The sample was placed on a horizontal quartz glass sample holder plate.

Attenuated Total Reflectance-Fourier-Transform Infrared Spectroscopy

Attenuated total reflectance-Fourier-transform infrared spectroscopy (ATR-FTIR) was performed using a Varian, Inc. 7000e step-scan spectrometer (Agilent Technologies, Santa Clara, CA, USA), using similar conditions reported by the authors (22,23). The particle powder was placed on the diamond ATR crystal, covered with a glass coverslip, and held in place with a specialized clamp. The ATR crystal and IR spectra were obtained at an 8 cm^{-1} spectral resolution between 700 and 4,000 cm^{-1}. The data were collected and analyzed using Varian Resolutions software.

Hot-Stage Microscopy

Using similar conditions reported by the authors (22,23), hot-stage microscopy (HSM) studies were completed using an Olympus BX51 polarized microscope (Olympus, Japan) equipped with an Instec STC200 heating unit and S302 hot stage (Boulder, CO, USA). The polarized light was filtered by a γ 530 nm U-TP530 filter lens. Powder samples were mounted on a cover glass and heated from 25°C to 250°C at a heating rate of 5°C min^{-1}. The heating program was controlled by WinTemp software, and images were digitally

captured *via* a SPOT Insight digital camera (Diagnostic Instruments, Inc., Sterling Heights, MI, USA).

Paclitaxel Loading Analysis by UV-VIS Spectroscopy

UV-VIS spectroscopy was used to determine the amount of paclitaxel loaded into the formulated particle systems. The particles were dissolved in methanol at 2 mg ml^{-1}, and 100 μl of each sample was transferred to a well of a UV-VIS-transparent 96-well plate. The absorbance of the samples was then read at a wavelength of 230 nm using a SynergyMx BioTek microplate reader and analyzed using the Gen5 2.00 software. Various concentrations of PTX were also dissolved in methanol and the corresponding absorbance intensities allowed for the creation of a calibration curve within the range of the PTX content in the particles. The paclitaxel encapsulation efficiency (EE) and loading were calculated as follows by Eqs. 1 and 2:

$$\text{Encapsulation efficiency (EE)} = \frac{\text{Actual mass of PTX}}{\text{Initial mass of PTX}} \times 100\% \quad (1)$$

$$\text{Drug loading} = \frac{\text{Actual mass of PTX}}{\text{Mass of particles}} \quad (2)$$

In Vitro Release of PTX from DPPC/DPPG Particles

In vitro drug release methods specifically for dry powder aerosol formulations have been reported recently by our group (24) and others (25–32). DPPC/DPPG particles with and without PTX were suspended in triplicate in a modified phosphate buffer comprised of PBS, 2.4 wt% Tween® 20, and 4 wt% Cremophor® EL to facilitate PTX solubility in an aqueous solution. The samples were incubated at 37°C and 150 rpm in an incubator shaker. At desired time points, aliquots were removed and centrifuged at 20,000×*g* for 10 min, and 100 μl of supernatant from each sample was transferred to a UV-transparent 96-well plate. The amount of paclitaxel in the sample at a given time was analyzed by measuring the absorbance as described in the previous section using a microplate reader.

In Vitro Aerosol Dispersion Performance by the Next Generation Impactor™

In accordance with US Pharmacopeia (USP) Chapter <601> specifications on aerosols (33) and our previously reported conditions (22,23), the *in vitro* aerosol dispersion properties of the dry powder particles were determined using the Next Generation Impactor™ (NGI™) with a stainless steel induction port (USP throat) attachment (NGI™ Model 170), equipped with specialized stainless steel NGI™ gravimetric insert cups (MSP Corporation, Shoreview, MN, USA). The NGI™ was coupled with a Copley TPK 2000 critical flow controller connected to a Copley HCP5 vacuum pump, and the airflow rate, Q, was measured and adjusted prior to each experiment using a Copley DFM 2000 flow meter (Copley Scientific, UK).

Glass fiber filters (55 mm, Type A/E, Pall Life Sciences, Exton, PA, USA) were placed in the gravimetric insert cups for stages 1 through 7 to minimize bounce or re-entrapment (34). Three hydroxypropyl methylcellulose (HPMC) hard capsules (size 3, Quali-V®, Qualicaps® Inc., Whitsett, NC, USA) were each loaded with 10 mg of powder. One capsule at a time was then loaded into a high-resistance FDA-approved DPI device, the Handihaler® (Boehringer Ingelheim, USA), and tightly inserted into the USP induction port. The NGI™ was run at a controlled flow rate (Q) of 60 l min^{-1} with a delay time of 10 s prior to the capsules being needle-pierced open by the Handihaler® mechanism, where the particles were then drawn into the impactor for 10 s. This was done with three capsules per particle sample for a total of 30 mg total per run. For each run, the amount of particles deposited onto each stage was determined gravimetrically by measuring the difference in mass of the glass filters after particle deposition. For Q=60 l min^{-1}, the effective aerodynamic cutoff diameters (D_{a50}) for each NGI™ impaction stage were calibrated by the manufacturer and stated as stage 1 (8.06 μm), stage 2 (4.46 μm), stage 3 (2.82 μm), stage 4 (1.66 μm), stage 5 (0.94 μm), stage 6 (0.55 μm), and stage 7 (0.34 μm). The fine particle dose (FPD), fine particle fraction (FPF), respirable fraction (RF), and emitted dose (ED) were calculated as follows by Eqs. 3–6:

$$\text{Fine particle dose (FPD)} = \text{Mass of particles deposited on stages 2 through 7} \quad (3)$$

$$\text{Fine particle fraction(FPF)} = \frac{\text{Fine particle dose}}{\text{Initial particle mass loaded into capsules}} \times 100\% \quad (4)$$

$$\text{Respirable fraction(RF)} = \frac{\text{Mass of particles deposited on stages 2 through 7}}{\text{Total particle mass on all stages}} \times 100\% \quad (5)$$

$$\text{Emitted dose(ED)} = \frac{\text{Initial mass in capsules}-\text{Final mass remaining in capsules}}{\text{Initial mass in capsules}} \times 100\% \quad (6)$$

The mass mean aerodynamic diameter (MMAD) and geometric standard deviation (GSD) of the aerosol dispersion profiles were determined using a Mathematica (Wolfram Research Inc., Champaign, IL) program written by Dr. Warren Finlay (35). All experiments were triplicated (n=3).

In Vitro Dose-Response Analysis of Lung Cancer Cells

The activity of the paclitaxel in the DPPC/DPPG particles was analyzed by measuring the response of lung adenocarcinoma cells at different concentrations of the drug. The A549 pulmonary cell line (ATCC, Manassas, VA) is a human alveolar epithelial lung adenocarcinoma cell line and is also used as a model of the alveolar type II pneumocyte cell in *in vitro* pulmonary drug delivery and metabolism studies. A549 pulmonary cells were grown in a growth medium including Dulbecco's modified Eagle's medium (DMEM), 10% (*v*/*v*) fetal bovine serum (FBS), Pen-Strep (100 U ml^{-1} penicillin, 100 μg ml^{-1} streptomycin), and Fungizone® (0.5 μg ml^{-1} amphotericin B, 0.41 μg ml^{-1} sodium deoxycholate) in a humidified incubator at 37°C and 5% CO_2. DMEM, Pen-Strep, and Fungizone® were obtained from Invitrogen (Grand Island, NY) whereas FBS was from Fisher Scientific (St. Louis, MO). A549 cells were seeded in 96-well plates at 7,500 cells ml^{-1} and 100 μl $well^{-1}$ and were allowed to attach overnight. The cells were then exposed to various concentrations of paclitaxel ranging from 0.005 to 5 μM in both raw PTX and particle formulations suspended in media. Raw PTX was dissolved in 0.1% (*v*/*v*) DMSO to facilitate solubility in the media. One hundred microliters of the drug or particle sample was added to each well. Seventy two hours after exposure, 20 μl of 10 mM resazurin was added to each well and incubated for 3 h. At this point, the fluorescence intensity of the resorufin produced by viable cells was detected at 520 nm (excitation) and 590 nm (emission) using the SynergyMx BioTek microplate reader described previously. The relative viability of each sample was calculated by Eq. 7:

$$\text{Relative viability}\,(\%) = \frac{\text{Sample fluorescence intensity}}{\text{Control fluorescence intensity}} \times 100\% \quad (7)$$

The corresponding IC50 values for paclitaxel in the samples were determined using www.readerfit.com.

In Vitro Cellular Uptake of Phospholipid Particles in Lung Cells

A549 pulmonary cells were seeded at 200,000 cells ml^{-1} (300 μl $well^{-1}$) in eight chamber slides and attached overnight. The cells were then exposed to 12 mg ml^{-1} of fluorescently labeled particles in media for 6 and 24 h at 37°C. The particles were 50PTX:50DPPC/DPPG particles with 1 mol% nitrobenzoxadiazole phosphatidylcholine (NBD-PC) fluorophore to allow for fluorescent imaging of the particles. After exposure, the particle solution was removed and the cells were washed twice with 200 mM glycine to remove any unbound particles, followed by a wash with PBS. The cells were then stained with 750 nM Lysotracker Blue and 5 μg ml^{-1} Hoescht 33342 (Life Technologies, Grand Island, NY) in PBS prior to imaging with a Nikon Elipse LV100 fluorescent microscope.

In Vitro Transepithelial Electrical Resistance Analysis Upon Particle Exposure to Lung Epithelial Cells

Calu-3 lung epithelial cells (ATCC, Manassas, VA), a human lung adenocarcinoma cell line derived from the bronchial submucosal airway region, were cultured similar to A549 cells but with Eagle's minimum essential medium (EMEM) instead of DMEM. The cells were seeded at 500,000 cells ml^{-1} in Transwells (0.4 μm polyester membrane, 12 mm for a 12-well plate) with 0.5 ml of media on the apical side and 1.5 ml of media on the basolateral side. After 2 days of growth, the media were removed from both sides and 400 μl of media was added to the basolateral side of the Transwells to facilitate air-interface culture (AIC) conditions. The TEER responses of the cells were measured starting at this time point with an Endohm 12 mm Culture Cup (World Precision Instruments, Sarasota, FL). For TEER measurement, 0.5 ml of media was added to the apical side of the Transwell 5 min before measurement and then immediately removed to return the cells to AIC conditions. After the TEER values reached 500 Ω cm^2 (indicating a confluent monolayer), the cells were exposed to 1 mg of DPPC/DPPG particles per well by a needle and syringe. TEER values were then recorded after exposure up to 5 days after particle treatment. The final data were then represented as the percent response of the control which was calculated using Eq. 8:

$$\text{TEER \% control} = \frac{\text{Sample TEER value}}{\text{Control TEER value}} \times 100\% \quad (8)$$

Statistical Analysis

All experiments were performed in at least triplicate (n=3). MYSTAT 12 for Windows (12.01.00) was used for t tests to determine any significance in observed data. A p value of <0.05 was considered statistically significant. The results are expressed as mean±standard deviation.

RESULTS

Morphology, Shape, and Size Analysis

Particle morphology and size were visualized *via* SEM. Figure 1 includes SEM micrographs of co-SD particles with varying SD rates and paclitaxel content. 0PTX:100DPPC/DPPG particles (without paclitaxel) were co-spray-dried at different rates to determine this effect on the particle systems. For both low P and med P pump rates (Fig. 1a and b, respectively), the particles exhibited sintering and agglomeration with very minimal particle formation for the low P sample. For samples made at the high P flow rate both with and without PTX, they were smooth, spherical, and uniform in shape. Table I shows the corresponding diameters for the high P samples, and while the size ranges from 1.07 to 1.38 μm, there is no difference in the size of the particles according to PTX loading. The sizes of low P and med P SD samples were not analyzed due to their agglomerated state.

Karl Fischer Coulometric Titration

The residual water content of co-SD samples and raw DPPG is shown in Table II. The water content of raw DPPC, DPPG, and PTX was 0.56%, 1.74%, and 0.49% (*w*/*w*), respectively, whereas the amount of water in the high P co-SD particles ranged from 1.44% to 4.23% (*w*/*w*) and decreased with increasing PTX loading. The water contents for raw

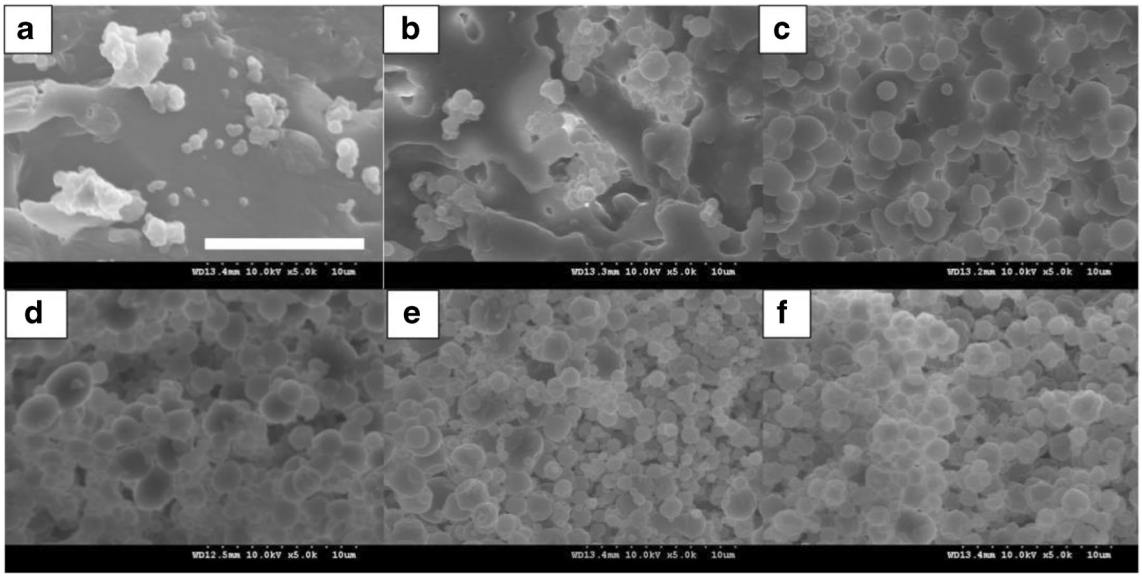

Fig. 1. SEM micrographs of co-spray-dried (co-SD) DPPC/DPPG particles with varying PTX content: **a** 0PTX:100DPPC/DPPG (low), **b** 0PTX:100DPPC/DPPG (med), **c** 0PTX:100DPPC/DPPG (high), **d** 25PTX:75DPPC/DPPG (high), **e** 50PTX:50DPPC/DPPG (high), and **f** 75PTX:25DPPC/DPPG (high). Magnification for all samples was ×10,000

DPPC and raw DPPG are in excellent agreement with our earlier reported values (36,37). Particle samples without PTX exhibited water content from 3.96% to 4.52% (*w*/*w*) with no discernible difference due to the spray-drying pump rate.

Differential Scanning Calorimetry

DSC thermograms for formulated particles and their corresponding raw counterparts can be seen in Fig. 2. Formulated 0PTX:100DPPC/DPPG particles exhibited a characteristic bilayer main phase transition phase, T_m, at ~72°C, confirming the miscibility of DPPC with DPPG, as would be expected and has been reported under different conditions (38). The low P and high P 0PTX samples exhibited a doublet peak at this transition whereas high P particles did not. There was no trend in the heat of fusion for 0PTX particles where these values were 29.1, 68.8, and 26.0 J g^{-1} for low P, med P, and high P, respectively. For 25PTX:75DPPC/DPPG particles, a crystal-to-gel (T_c) bilayer phase transition occurred at 48.6°C, main phase transition at 67.5°C, and degradation at 219°C. No peaks were present in the phospholipid range (40–70°C) for 50PTX:50DPPC/DPPG and 75PTX:25DPPC/DPPG particles; however, degradation occurred at 207.4°C and 209.4°C, respectively. Furthermore, the latter system exhibited a glass transition peak (T_g) at 145.9°C. The T_g is a second-order solid-state phase transition from the amorphous glass to the amorphous rubber. There were no measurable melting peaks for any of the formulated particles corresponding to PTX. For the raw materials, DPPC exhibited a crystal-to-gel (T_c) bilayer phase transition at 47.1°C, a pre-transition peak corresponding to a gel-to-ripple (T_p) phase at 67.0°C, and bilayer main phase transition (T_m) to the liquid crystalline phase at 72.0°C. Raw DPPC went through the bilayer main phase transition at 79.6°C. Raw PTX exhibited a glass transition phase at 149.0°C, melting at 212°C, and degradation at 223.6°C.

X-ray Powder Diffraction

X-ray powder diffraction (XRPD) diffractograms (Fig. 3) showed the presence of a strong peak at 21° 2θ for both raw DPPC, formulated 0PTX:100DPPC/DPPG, and formulated 25PTX:75DPPC/DPPG, which corresponds to the presence of the phospholipid bilayer structure (39). The intensity of the peak at 21° 2θ decreased with increasing PTX content

Table I. List of Co-spray-dried (co-SD) Formulation Compositions, Their Corresponding Outlet Temperatures During Spray-drying, Particle Size, Paclitaxel (PTX) Loading, and PTX Encapsulation Efficiency (EE) and Loading. (n=3, ave±SD)

Co-SD system composition (molar ratio)	Outlet T (°C)	Diameter (μm)	PTX EE (%)	PTX loading (mg/mg)
0PTX:100DPPC/DPPG (low P)	95	n/a	n/a	0
0PTX:100DPPC/DPPG (med P)	69	n/a	n/a	0
0PTX:100DPPC/DPPG (high P)	42	1.16±0.06	n/a	0
25PTX:75DPPC/DPPG (high P)	49	1.11±0.09	107.9±1.2	0.301±0.003
50PTX:50DPPC/DPPG (high P)	50	1.07±0.08	101.5±1.8	0.525±0.009
75PTX:25DPPC/DPPG (high P)	56	1.10±0.05	106.3±2.0	0.825±0.016

DPPC dipalmitoylphosphatidylcholine, *DPPG* dipalmitoylphosphatidylglycerol

Table II. List of Water Content Values for Co-spray-dried (co-SD) Formulations and Their Raw Counterparts. (n=3, ave±SD)

Co-SD system composition (molar ratio)	Water content % (w/w)
0PTX:100DPPC/DPPG (low P)	3.86±0.21
0PTX:100DPPC/DPPG (med P)	4.45±0.81
0PTX:100DPPC/DPPG (high P)	4.23±0.39
25PTX:75DPPC/DPPG (high P)	2.89±0.46
50PTX:50DPPC/DPPG (high P)	3.12±0.20
75PTX:25DPPC/DPPG (high P)	1.44±0.34
Raw DPPC	1.74±0.15
Raw DPPG	0.56±0.51
Raw PTX	1.45±0.71

PTX paclitaxel, *DPPC* dipalmitoylphosphatidylcholine, *DPPG* dipalmitoylphosphatidylglycerol

for the formulated particles. Raw DPPG showed the presence of sharp peaks at 20 and 22.5° 2θ, but not in the formulated particles. The many peaks in raw PTX indicated that it was initially crystalline, but the smooth peaks for formulated particles indicate the PTX present is amorphous throughout the particle structure.

Attenuated Total Reflectance-Fourier-Transform Infrared Spectroscopy

Formulated particles and their raw counterparts underwent ATR-FTIR analysis to determine the functional groups present in the system, as shown in Fig. 4. Many of the characteristic peaks of raw DPPG were visible in the SD formulated particles although their intensities decreased with increasing PTX content. In particular, strong peaks were present due to –CH_2 antisymmetrical stretching (2,924 cm^{-1}), –CH_3 symmetrical stretching (2,870 cm^{-1}), C=O ester stretching (1,720–35 cm^{-1}), –CH_2 deformation (1,465 cm^{-1}), P=O stretching (1,250–1,350 cm^{-1}), –C–C– bonds (1,050–1,150 cm^{-1}), and –$N^+(CH_3)_3$ antisymmetrical stretching (964 cm^{-1}). A broad peak between 3,200 and 3,400 cm^{-1} was present for raw DPPC and 0PTX:100DPPC/DPPG due to the presence of water. While raw PTX exhibited similar peaks to the formulated particles, it in turn showed doublet peaks at 1,720–1,735 and 1,650 cm^{-1}.

Hot-Stage Microscopy

Representative HSM micrographs of the formulated co-SD particles are shown in Fig. 5. All samples initially showed

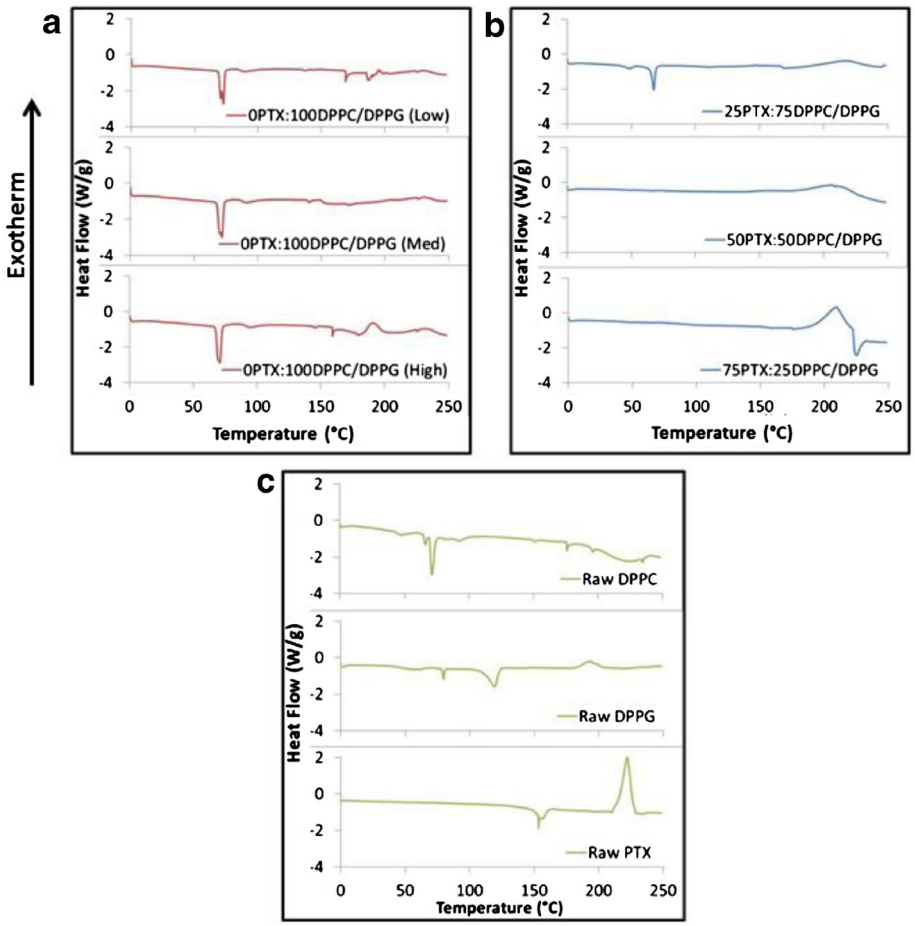

Fig. 2. DSC thermograms of **a** co-spray-dried (co-SD) DPPC/DPPG particles (75:25 M ratio) with varying pump rates (low, med, and high), **b** co-SD particles containing DPPC and DPPG with varying PTX content, and **c** their raw counterparts

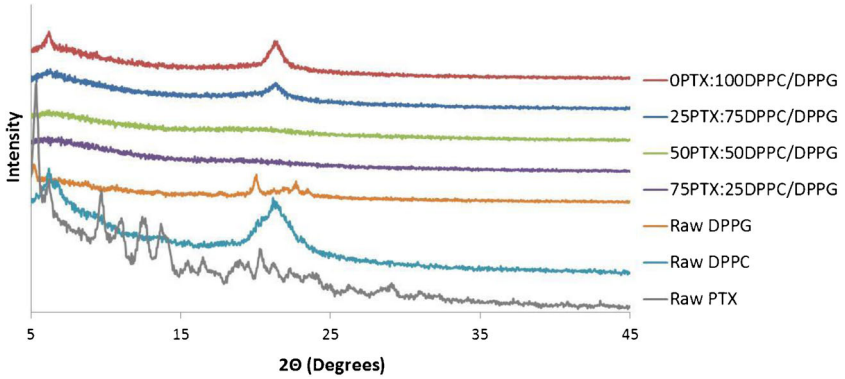

Fig. 3. X-ray powder diffractograms of co-SD DPPC/DPPG particles with varying PTX content and their corresponding raw components

dark agglomerates lacking birefringency until they appeared to melt, which indicated a non-crystalline, amorphous material. For 0PTX:100DPPC/DPPG, melting was visualized starting at 90°C by the formation of liquid droplets whereby the samples then demonstrated birefringency. The 25PTX:75DPPC/DPPG and 75PTX:25DPPC/DPPG particles appeared to melt at around 145°C and while 25PTX showed birefringency, 75PTX did not. This was also seen for the 50PTX:50DPPC/DPPG sample (data not shown).

Paclitaxel Loading Analysis *via* UV-Vis Spectroscopy

The formulated co-SD particles containing PTX were analyzed for the PTX encapsulation efficiency (EE) and loading *via* UV-VIS spectroscopy. As shown in Table I, all of the samples had EE values slightly over 100% in the range of 101.5–107.9%. The PTX loading for 25PTX:75DPPC/DPPG, 50PTX:50DPPC/DPPG, and 75PTX:25DPPC/DPPG were 0.301, 0.525, and 0.825 mg PTX per milligram particle, respectively.

In Vitro Release Studies of PTX from DPPC/DPPG Particles

In vitro release of paclitaxel was evaluated with the particles suspended in modified PBS medium (*i.e.*, ~1 mg particles in 1 ml release medium) with Cremophor® and Tween to facilitate paclitaxel solubility, as PTX has a very low aqueous solubility. As shown in Fig. 6, while there is an initial release evident, it is very minimal for all three systems containing PTX (less than 15%). After 21 days, 37%, 53%, and 66% of the paclitaxel was released from 75PTX:25DPPC/DPPG, 50PTX:50DPPC/DPPG, and 25PTX:75DPPC/DPPG particles, respectively.

In Vitro Aerosol Dispersion Performance *via* Next Generation Impactor™

The aerosol properties of the formulated co-SD particles were evaluated using an NGI™ coupled with a Handihaler® DPI device. MMAD and GSD values increased with decreasing PTX content, as seen in Table III. The FPF values also increased significantly upon the addition of PTX where unloaded particles had a FPF of 35.8% and loaded particles had FPFs ranging from 77.6 to 86.7% (there was no noticeable trend due to PTX loading). The RF values ranged from 51.3% to 63.8% and ED values from 80.0% to 90.7% but there were no noticeable trends due to the extent of PTX loading. Figure 7 demonstrates the actual aerosol dispersion performance of the formulated dry powder aerosols by showing the percent deposition of the particles on each

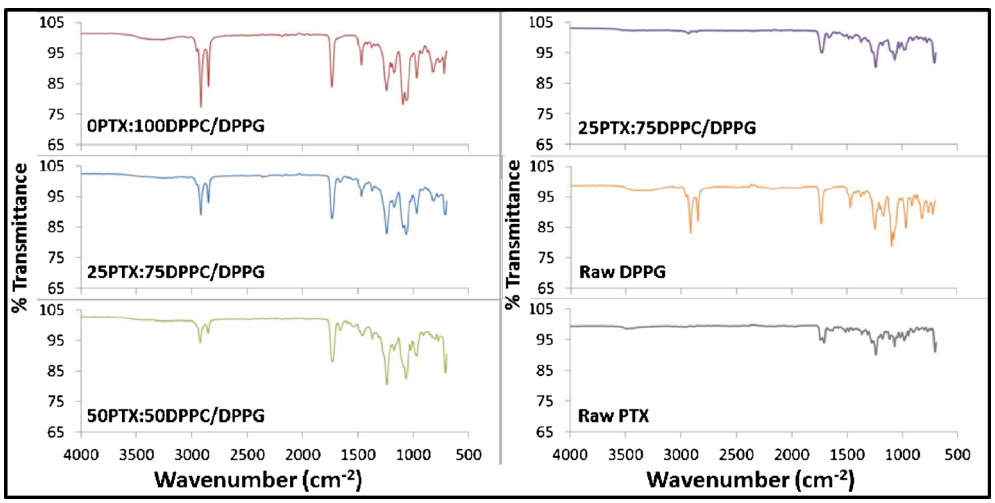

Fig. 4. Representative ATR-FTIR spectra of co-SD PTX:DPPC/DPPG particles in comparison to raw DPPC and raw paclitaxel

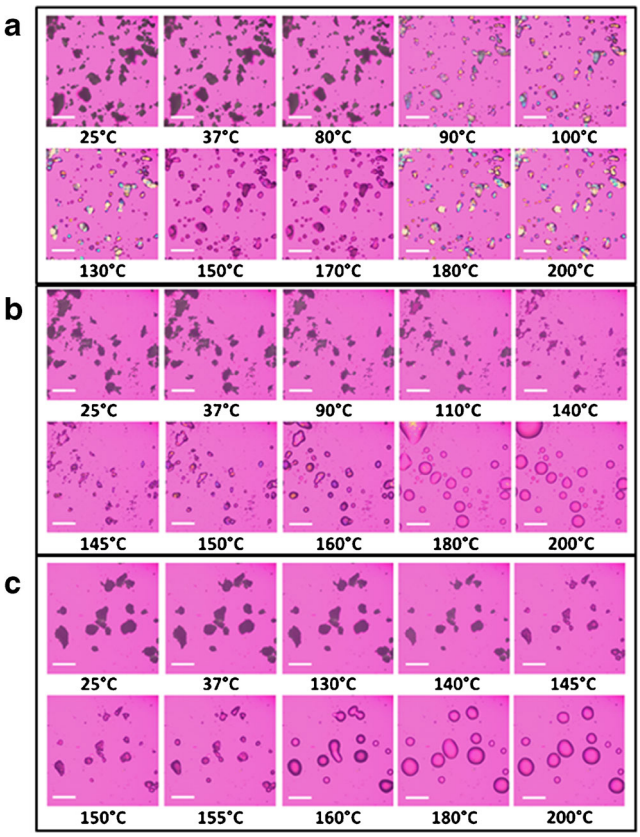

Fig. 5. Representative HSM micrographs of co-SD particles comprised of **a** co-SD 0PTX:100DPPC/DPPG, **b** co-SD 25PTX:75DPPC/DPPG, and **c** co-SD 75PTX:25DPPC/DPPG (*scale bar*=3 mm)

NGI™ stage. Aerosol deposition was measurable on all of the stages, and in particular, deposition on the lower stages of stage 2 to stage 7 (lowest stage) is observed. The amount of particles deposited on the lower stages (especially stages 4 through 6) increased with increasing PTX particle composition.

In Vitro Drug Dose-Response Analysis of Lung Cancer Cells

The chemotherapeutic cytotoxic activity of paclitaxel encapsulated in the formulated particles was evaluated by exposing A549 cells to the different particle systems in comparison to raw PTX. Figure 8 shows the dose-response curves which indicate that the PTX in the formulated particles were more toxic than raw PTX 48 h after exposure. Particles without paclitaxel (0PTX:100DPPC/DPPG) had a relative viability of 94% (data not shown) which was significantly different from the control with no particles (p=0.045). The effectiveness of the particles was also evaluated by the IC50 values which were 0.0109, 0.0464, 0.0266, and 0.4174 μM of paclitaxel, as shown in Table IV.

In Vitro Cellular Uptake of Phospholipid Particles in Lung Cells

A549 cells were exposed to 50PTX:50DPPC/DPPG particles loaded with 1 mol% NBD-PC fluorophore so that they could be imaged *via* fluorescent microscopy. After 6 h of exposure at 37°C, there was minimal particle uptake evident as seen in Fig. 9. The few particles that were visible were likely stuck to the microscope slide area around the cells. There was no noticeable uptake in either the nucleus or cytoplasm of the cells. For the 24-h exposure, there was noticeably less cytoplasm staining which was likely due to the amount of cell death present in the cells due to the paclitaxel present after 24 h since cells release their cytoplasm upon apoptosis (40). There were also fewer particles present in all of the pictures indicating minimal uptake of the particles. A control with no drug (0PTX:100DPPC/DPPG) was also evaluated with results similar to that with drug (data not shown).

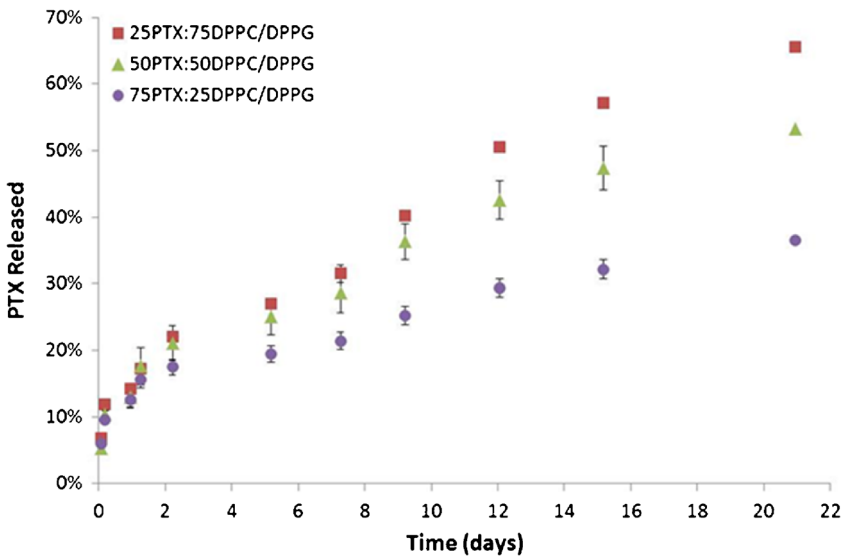

Fig. 6. *In vitro* paclitaxel release from co-SD PTX-loaded DPPC/DPPG particles in modified PBS medium over 21 days at 37°C. (n=3, ave±SD)

Table III. *In Vitro* Aerosol Performance Using the Next Generation Impactor™ for Co-spray-dried (co-SD) Aerosol Systems Including Mass Median Aerodynamic Diameter (MMAD), Geometric Standard Deviation (GSD), Fine Particle Fraction (FPF), Respirable Fraction (RF), and Emitted Dose (ED). (n=3, ave±SD)

Co-SD system composition (molar ratio)	MMAD (μm)	GSD (μm)	FPF (%)	RF (%)	ED (%)
0PTX:100DPPC/DPPG	10.4±1.3	4.5±1.0	35.8±3.9	53.6±1.7	80.0±6.7
25PTX:75DPPC/DPPG	3.3±0.5	2.2±0.6	81.6±8.8	51.3±6.1	82.0±6.6
50PTX:50DPPC/DPPG	1.9±0.1	1.9±0.1	86.7±2.6	63.8±0.1	81.6±8.2
75PTX:25DPPC/DPPG	2.3±0.2	2.1±0.4	77.6±2.4	58.2±1.2	90.7±7.1

PTX paclitaxel, *DPPC* dipalmitoylphosphatidylcholine, *DPPG* dipalmitoylphosphatidylglycerol

In Vitro Transepithelial Electrical Resistance Analysis upon Particle Exposure to Lung Epithelial Cells

TEER measurements were completed on Calu-3 cells to determine the effect of PTX-loaded formulated particles on cells exposed to air-interface culture (AIC) conditions. The presence of an effective cell monolayer was confirmed by steady TEER values (at least 500 Ω cm^2) after 5 days of culturing in AIC conditions and the presence of a cell monolayer *via* light microscopy (data not shown). Starting 2 h after exposure to the formulated particles, cells at AIC were measured for TEER (up to 5 days after treatment). As seen in Fig. 10, the TEER values remained statistically the same as those of the control both before and after treatment (p values >0.05).

DISCUSSION

This comprehensive study illustrates the physicochemical and *in vitro* properties of rationally designed paclitaxel-loaded DPPC/DPPG co-SD particles *via* organic solution advanced spray-drying (SD). This is the first time surfactant-based dry powder particles have been produced with encapsulated PTX. The approach in using micron-sized surfactant-based dry powder particles offers advantages over systems such as aerosolized liposomes, larger dry powder microparticles, and nanoparticles (41). In particular, the size of the described particles is within a size range to allow for effective alveolar deposition while also providing enhanced stability during long-term storage. A more detailed description of these systems follows.

Systematic experimental design resulted in the development and optimization of four practical particle systems, which included three systems loaded with paclitaxel (25, 50, and 75 mol%) and one without. The study strived to elucidate the effects of the presence of the pump rate, DPPG, and paclitaxel loading, especially on the aerosol properties of the system. As we have described previously, dilute organic solution SD results in smaller primary droplet sizes within the cyclone due to the lower surface tension of the solvent in comparison to water. This method also eliminates the need for water and thereby minimizes the residual water content in the final powder, thereby improving aerosol dispersion performance and stability.

SEM analysis showed that the particles spray-dried at the highest pump rate (high P) exhibited an ideal size range (around 1 μm), which is comparable to DPPC/DPPE-PEG dry powder particles. The size of the particles is paramount in ensuring targeted delivery to specific regions of the lung, and the particles in the reported size range are capable of

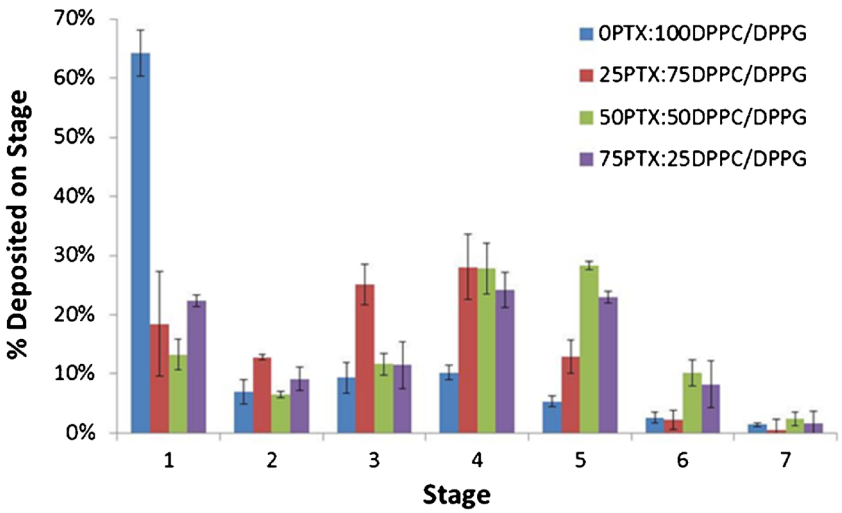

Fig. 7. *In vitro* aerosol dispersion performance as percent deposited on each stage of the Next Generation Impactor™ (NGI™) for spray-dried (SD) and co-spray-dried (co-SD) particles containing DPPC and DPPG with varying PTX content. For Q=60 l min^{-1}, the effective cutoff diameters (D_{a50}) for each NGI™ impaction stage are as follows: stage *1* (8.06 μm), stage *2* (4.46 μm), stage *3* (2.82 μm), stage *4* (1.66 μm), stage *5* (0.94 μm), stage *6* (0.55 μm), and stage *7* (0.34 μm). (n=3, ave±SD)

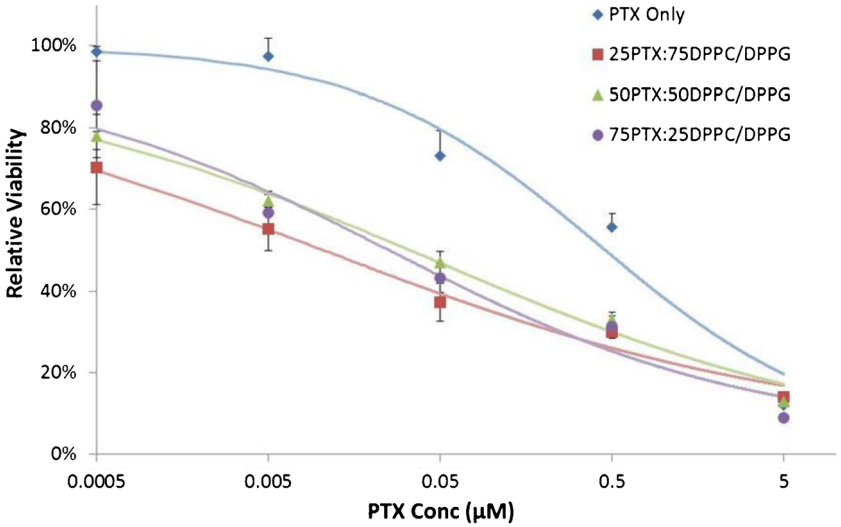

Fig. 8. *In vitro* drug dose-response curves for A549 cells exposed to DPPC/DPPG particle formulations with varying concentrations of PTX after 48 h of exposure at 37°C. (n=3, ave±SD)

delivering a payload to the deep lung (42,43). Many other systems often describe larger particles, such as alginate microparticles containing PTX which had MMAD values of 5.9 μm, which is too large for alveolar deposition (44). While all of the high P samples produced workable particles, those formulated at the low and medium pump rates were agglomerated with visible sintering present. After determining the superior properties of the particles formulated at the highest pump rate (30 ml min^{-1}), further formulations were made and characterized at this condition.

XRPD and DSC analysis showed that the formulated particles demonstrated the presence of the lipid bilayer structure (multilamellar) as evidence of the signature peaks for XRPD and characteristic bilayer phase transition values in DSC thermograms (38,45). XRPD diffractograms were the same for both raw DPPC and the formulated particles, with little similarity to raw DPPG, which is likely due to the significant presence of DPPC *versus* the latter. The characteristic peak at 21° 2θ proved the presence of the lipid bilayer(s), and the intensity of this peak decreased with increasing PTX content. DSC thermograms proved the presence of the lipid bilayer for formulated particles without paclitaxel with similar T_m values irrespective of the pump rate. This bilayer phase transition was also present in the 25PTX:75DPPC/DPPG formulated particle system; however, no peak was observed for the particles with higher PTX loading. This could be due to the limitation in phospholipid bilayer detection in regard to the concentration for the DSC system used for this analysis. The relationship between the outlet temperatures from the spray-drying process and the endothermic peak values due to the phase transition of the lipid bilayers was likely a significant factor in the successful formulation of multilamellar particles using the highest pump rate. The outlet temperatures for the low and medium pump rate were 92°C and 69°C, respectively, which were above the phase transition temperatures of the formulated particles, resulting in improper formation and agglomeration. The higher pump rate decreased the outlet temperature to 56°C or lower, allowing for the formulation of ideally sized, smooth particles. Furthermore, since the particles containing high amounts of paclitaxel were spray-dried and consequently contained low amounts of water and exhibited amorphous characteristics, they offer increased physical stability for long-term storage considerations (46).

Table IV. IC50 Values for A549 Cells Exposed to Co-SD DPPC/DPPG Particles Containing PTX *Versus* Free PTX After 48 h of Exposure at 37°C

System composition (molar ratio)	PTX IC50 (μM)
Free PTX	0.4174
25PTX:75DPPC/DPPG	0.0109
50PTX:50DPPC/DPPG	0.0266
75PTX:25DPPC/DPPG	0.0464

PTX paclitaxel, *DPPC* dipalmitoylphosphatidylcholine, *DPPG* dipalmitoylphosphatidylglycerol

HSM enabled the visualization of the particles as a function of temperature and confirmed the phase transitions of the formulated particles. It also demonstrated the stability of the particles at room and physiological temperatures. ATR-FTIR analysis of particles in the solid state confirmed the presence of DPPC and DPPG where appropriate through the signature peaks of each of these materials without destruction of the particles that can occur using other FTIR methods. Organic spray-drying resulted in low water content of the particles, which is necessary for effective particle delivery since residual water can impede the dispersion of dry particles during aerosolization (47,48). These values were low for inhalation applications, which is a novel advantage in this method of spray-drying.

Excellent aerosol dispersion performance and performance parameters were demonstrated using the NGI™ coupled with the Handihaler® DPI device. The results indicated that the formulated particles would be optimal for predominant deposition into the deep lung region, particularly for the paclitaxel-loaded formulations. The

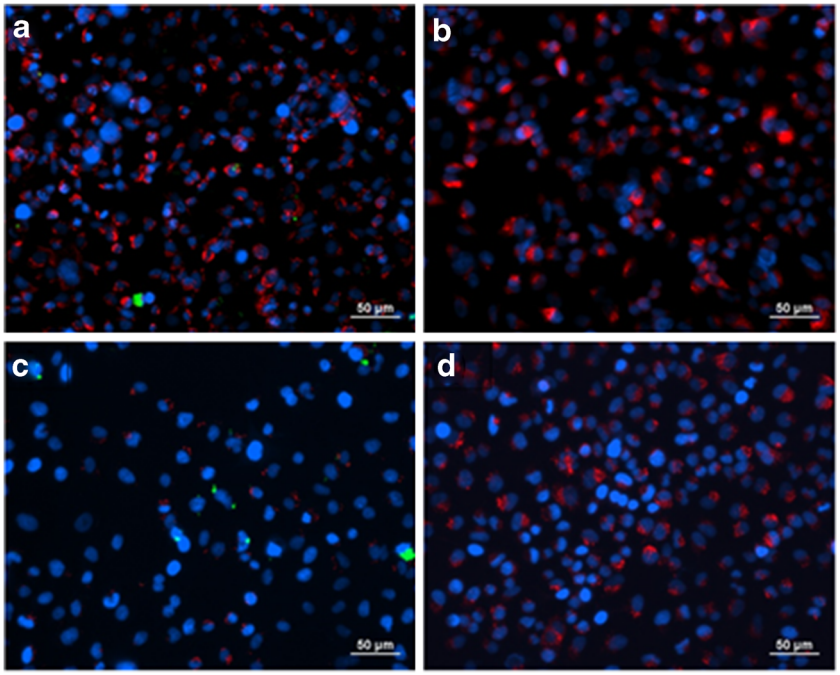

Fig. 9. Merged fluorescent micrographs of A549 lung adenocarcinoma cells exposed to co-SD 50PTX:50DPPC/DPPG formulated particles loaded with 1 mol% NBD-PC (fluorophore) for 6 h (**a** and **b**, *top row*) and 24 h (**c** and **d**, *bottom row*) at 37°C: **a** and **c** show the micrographs of cells that were exposed to particles, and **b** and **d** are control cells with no particle exposure. The nucleus (*blue*) and cytoplasm (*red*) were fluorescently labeled after particle exposure and washing

MMAD values were within the range (1–5 μm) necessary to deposit predominantly in the middle and deep lung regions by sedimentation due to gravitational settling (3,49–51). Furthermore, the presence of DPPG in the particle formulations enhanced the aerosol performance, particular in regard to the FPF values which increased from a range of 65.8–75.4% without DPPG to 77.6–86.7% (Table III) for the current particle systems. This latter data is from our previous work with particles also spray-dried with 25, 50, and 75 mol% loading of paclitaxel with DPPC only (*i.e.*, no DPPG) (22). While the FPF values increased for the current formulations compared to PTX:DPPC particles without DPPG, the RF and ED values remained similar overall indicating the potential for these systems to more efficiently deposit in the lower regions of the lung while providing high local concentration at the target site.

In vitro analysis of the formulated particles confirmed many important findings in paclitaxel loading and release, paclitaxel cytotoxic activity, and particle safety *via* pulmonary cellular viability analysis and TEER measurements. Overall, all systems exhibited very high loading of paclitaxel which allows for less particle mass to be delivered to the lung in relation to the actual amount of paclitaxel needed. Controlled PTX release over several weeks was clearly demonstrated for the co-SD PTX DPPC/DPPG powders. PTX was successfully released from all of the particle systems with the percentage of drug being released increasing with less paclitaxel amount although approximately the same amount of drug was

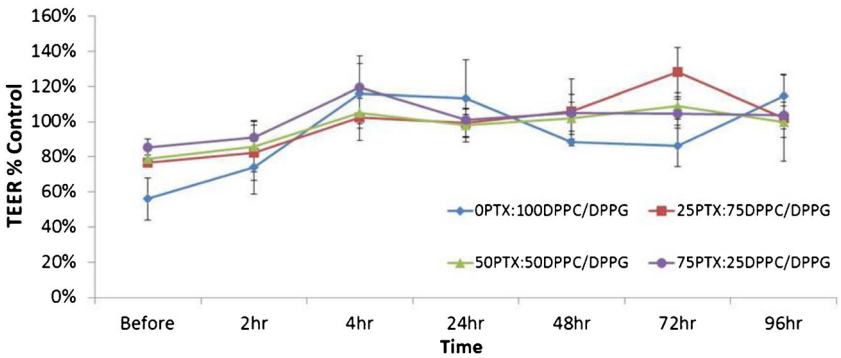

Fig. 10. Transepithelial electrical resistance (*TEER*) analysis of Calu-3 lung epithelial cells exposed to co-SD DPPC/DPPG particles containing paclitaxel (*PTX*) in air-interface culture (*AIC*) conditions at 37°C. TEER percent control values were calculated as reference to control cells not exposed to particles but grown in AIC conditions. (n=3, ave±SD)

released for all systems mass-wise (data not shown). Pulmonary cellular viability analysis indicated that the paclitaxel was still active and effective after encapsulation *via* co-spray-drying and actually exhibited enhanced cytotoxicity on lung cancer cells from co-SD DPPC/DPPG particles. TEER analysis showed the co-SD particles to be safe for pulmonary delivery in regard to epithelial lining integrity. The findings reported here indicate the significant potential of these phospholipid particles to be utilized to effectively deliver chemotherapeutics for the treatment of lung cancer in addition to many other different types of therapeutics as inhaled dry powder aerosols.

CONCLUSIONS

This comprehensive and systematic study reports for the first time on rationally designed lung surfactant-mimic DPPC/DPPG dry powder particles containing paclitaxel (a first-line lung cancer chemotherapeutic drug) for targeted pulmonary delivery as high-performing microparticulate/nanoparticulate dry powder inhalers. These multifunctional respirable therapeutic particles exhibited high *in vitro* aerosol performance, high drug loading, sustained drug release over weeks, and enhanced PTX *in vitro* cytotoxicity on lung cancer cells, further emphasizing their ability to deliver a chemotherapeutic drug for the treatment of lung cancer. *In vitro* cellular characterization with fluorescence microscopy imaging on lung cancer cells confirmed the cytotoxic chemotherapeutic activity of paclitaxel and the safety of the particles *via* pulmonary cell viability analysis and transepithelial electrical resistance (TEER) testing at air-interface conditions.

ACKNOWLEDGMENTS

The authors gratefully acknowledge financial support from the National Institutes of Health (NIH)-National Cancer Institute (NCI) Grant Number R25CA153954 and an NIH-NCI Cancer Nanotechnology Training Center (CNTC) Postdoctoral Traineeship awarded to SAM. The content is solely the responsibility of the authors and does not necessarily represent the official views of the NCI or the NIH. The authors thank Dr. Tonglei Li for XRPD and HSM access and Dr. J. Zach Hilt for ATR-FTIR access.

Conflict of Interest No conflicts of interest exist.

REFERENCES

1. American Cancer Society. Cancer Facts & Figures. In. Atlanta: American Cancer Society; 2013. p. 4–8.
2. Mansour HM, Rhee Y-S, Wu X. Nanomedicine in pulmonary delivery. Int J Nanomedicine. 2009;4:299–319.
3. Carvalho TC, Carbalho SR, McConville JT. Formulations for pulmonary administration of anticancer agents to treat lung malignancies. J Aerosol Med Pulm Drug Deliv. 2011;24(2):61–80.
4. Gagnadoux F, Hureaux J, Vecellio L, Urban T, Le Pape A, Valo I, *et al*. Aerosolized chemotherapy. J Aerosol Med Pulm Drug Deliv. 2008;21(1):61–9.
5. Sharma S, White D, Imondi A, Placke ME, Vail DM, Kris MG. Development of inhalation agents for oncologic use. J Clin Oncol. 2001;19(6):1839–47.
6. Gautam A. Targeted delivery of therapeutics by aerosol for cancer of the lung. Curr Cancer Drug Targets. 2003;3:57.
7. Haigentz MJ, Perez-Soler R. Chemopreventative therapeutics: inhalation therapies for lung cancer and bronchial premalignancy. Meth Mol Med. 2003;75:771–80.
8. Rubin BK. Mucus and mucins. Otolaryngol Clin N Am. 2010;43(1):27.
9. Laube BL, Janssens HM, de Jongh FHC, Devadason SG, Dhand R, Diot P, *et al*. What the pulmonary specialist should know about inhalation therapies. Eur Respir J. 2011;37:1308–31.
10. Weers JG, Bell J, Chan HK, Cipolla D, Dunbar C, Hickey AJ, *et al*. Pulmonary formulations: what remains to be done? J Aerosol Med Pulm Drug Deliv. 2010;23:S5–S23.
11. Labiris NR, Dolovich MB. Pulmonary drug delivery. Part II: The role of inhalant delivery devices and drug formulation in therapeutic effectiveness of aerosolized medications. Br J Clin Pharmacol. 2003;56:600–12.
12. Chow AHL, Tong HHY, Chattopadhyay P, Shekunov BY. Particle engineering for pulmonary drug delivery. Pharm Res. 2007;24(3):411–37.
13. Willis L, Hayes D, Mansour HM. Therapeutic liposomal dry powder inhalation aerosols for targeted lung delivery. Lung. 2012;190(3):251–62.
14. Eldar-Boock A, Miller K, Sanchis J, Lupu R, Vicent MJ, Satchi-Fainaro R. Integrin-assisted drug delivery of nano-scaled polymer therapeutics bearing paclitaxel. Biomaterials. 2011;32:3862–74.
15. Gill KK, Nazzal S, Kaddoumi A. Paclitaxel-loaded PEG5000-DSPE micelles as pulmonary delivery platform: formulation characterization, tissue distribution, plasma pharmacokinetics and toxicological evaluation. Eur J Pharm Biopharm. 2011;79:276–84.
16. Alipour S, Montaseri H, Tafaqhodi M. Preparation and characterization of biodegradable paclitaxel loaded alginate microparticles for pulmonary delivery. Colloids Surf B: Biointerfaces. 2010;81(2):521–9.
17. Mansour HM, Rhee YS, Park CW, DeLuca PP. Lipid nanoparticulate drug delivery and nanomedicine. In: Moghis A, editor. Lipids in nanotechnology. Urbana: American Oil Chemists Society (AOCS) Press; 2011. p. 221–68.
18. Jobe AH. Pulmonary surfactant therapy. N Engl J Med. 1993;328(12):861–8.
19. Labiris NR, Dolovich MB. Pulmonary drug delivery. Part I: Physiological factors affecting therapeutic effectiveness of aerosolized medications. J Clin Pharmacol. 2003;56:588–99.
20. Forbes B, Ehrhardt C. Human respiratory epithelial cell culture for drug delivery applications. Eur J Pharm Biopharm. 2005;60(2):193–205.
21. Grainger CI, Greenwell LL, Lockley DJ, Martin GP, Forbes B. Culture of Calu-3 cells at the air interface provides a representative model of the airway epithelial barrier. Pharm Res. 2006;23(7):1482–90.
22. Meenach SA, Anderson KW, Hilt JZ, McGarry RC, Mansour HM. Characterization and aerosol dispersion performance of advanced spray-dried chemotherapeutic PEGylated phospholipid particles for dry powder inhalation delivery in lung cancer. Eur J Pharm Sci. 2013;49(4):699–711.
23. Meenach SA, Vogt FG, Anderson KW, Hilt JZ, McGarry RC, Mansour HM. Design, physicochemical characterization, and optimization of organic solution advanced spray-dried inhalable dipalmitoylphosphatidylcholine (DPPC) and dipalmitoylphosphatidylethanolamine poly(ethylene glycol) (DPPE-PEG) microparticles and nanoparticles for targeted respiratory nanomedicine delivery as dry powder inhalation aerosols. Int J Nanomedicine. 2013;8:275–93.
24. Park CW, Li X, Vogt FG, Hayes DJ, Zwischenberger JB, Park ES, *et al*. Advanced spray dried design, physicochemical characterization and aerosol dispersion performance of vancomycin and clarithromycin multifunctional controlled release particles for targeted respiratory delivery as dry powder inhalation aerosols. Int J Pharm. 2013;455(1–2):374–92.
25. O'Hara P, Hickey AJ. Respirable PLGA microspheres containing rifampicin for the treatment of tuberculosis: manufacture and characterization. Pharm Res. 2000;17(8):955–61.
26. Sung JC, Padilla DJ, Garcia-Contreras L, VerBerkmoes JL, Durbin D, Peloquin CA, *et al*. Formulation and pharmacokinetics of

self-assembled rifampicin nanoparticle systems for pulmonary delivery. Pharm Res. 2009;26(8):1847–55.
27. Salama RO, Traini D, Chan H-K, Young PM. Preparation and characterisation of controlled release co-spray dried drug–polymer microparticles for inhalation 2: evaluation of in vitro release profiling methodologies for controlled release respiratory aerosols. Eur J Pharm Biopharm. 2008;70:145–52.
28. Son Y-J, McConville JT. Preparation of sustained release rifampicin microparticles for inhalation. J Pharm Pharmacol. 2012;64:1291–302.
29. Son Y-J, McConville JT. Development of a standardized dissolution test method for inhaled pharmaceutical formulations. Int J Pharm. 2009;382:15–22.
30. El-Sherbiny IM, McGill S, Smyth HDC. Swellable microparticles as carriers for sustained pulmonary drug delivery. J Pharm Sci. 2010;99(5):2343–56.
31. El-Sherbiny IM, Smyth HDC. Biodegradable nano-micro carrier systems for sustained pulmonary drug delivery: (I) self-assembled nanoparticles encapsulated in respirable/swellable semi-IPN microspheres. Int J Pharm. 2010;395:132–41.
32. El-Sherbiny IM, Smyth HDC. Controlled release pulmonary administration of curcumin using swellable biocompatible microparticles. Mol Pharm. 2012;9:269–80.
33. <601> Aerosols, nasal sprays, metered-dose inhalers, and dry powder inhalers monograph. In. USP 29-NF 24 The United States Pharmacopoeia and The National Formulary: The Official Compendia of Standards. Rockville, MD: The United States Pharmacopeial Convention, Inc.; 2006. p. 2617–2636.
34. Edwards DA, Ben-Jebria A, Langer R. Recent advances in pulmonary drug delivery using large, porous inhaled particles. J Appl Physiol. 1998;85(2):379–85.
35. Finlay W. The ARLA respiratory deposition calculator. 2010. Available from: http://www.mece.ualberta.ca/arla/impactor_mmad_calculator.html.
36. Wu X, Hayes DJ, Zwischenberger JB, Kuhn RJ, Mansour HM. Design and physicochemical characterization of advanced spray-dried tacrolimus multifunctional particles for inhalation. Drug Des Dev Ther. 2013;7:59–72.
37. Wu X, Zhang W, Hayes DJ, Mansour HM. Physicochemical characterization and aerosol dispersion performance of organic solution advanced spray-dried cyclosporine A multifunctional particles for dry powder inhalation aerosol delivery. Int J Nanomedicine. 2013;8:1269–83.
38. Mansour H, Wang DS, Chen CS, Zografi G. Comparison of bilayer and monolayer properties of phospholipid systems containing dipalmitoylphosphatidylglycerol and dipalmitoylphosphatidylinositol. Langmuir. 2001;17(21):6622–32.
39. Alves GP, Santana MHA. Phospholipid dry powders produced by spray drying processing: structural, thermodynamic and physical properties. Powder Technol. 2004;145:139–48.
40. Elmore S. Apoptosis: a review of programmed cell death. Toxicol Pathol. 2007;35(4):495–516.
41. Hitzman CJ, Elmquist WF, Wattenberg LW, Wiedmann TS. Development of a respirable, sustained release microcarrier of 5-fluorouracil I: in vitro assessment of liposomes, microspheres, and lipid coated nanoparticles. J Pharm Sci. 2006;95(5):1114–26.
42. Sung JC, Pulliam BL, Edwards DA. Nanoparticles for drug delivery to the lungs. Trends Biotechnol. 2007;25(12):563–70.
43. Azarmi S, Roa WH, Lobenberg R. Targeted delivery of nanoparticles for the treatment of lung diseases. Adv Drug Deliv Rev. 2008;60:863–75.
44. Hureaux J, Lagarce F, Gagnadoux F, Vecellio L, Clavreul A, Roger E, *et al*. Lipid nanocapsules: ready-to-use nanovectors for the aerosol delivery of paclitaxel. Eur J Pharm Biopharm. 2009;73(2):239–46.
45. Mansour HM, Zografi G. Relationships between equilibrium spreading pressure and phase equilibria of phospholipid bilayers and monolayers at the air-water interface. Langmuir. 2007;23:3809–19.
46. Vehring R, Foss WR, Lechuga-Ballesteros D. Particle formation in spray drying. J Aerosol Sci. 2007;38(7):728–46.
47. Hickey AJ, Mansour HM, Telko MJ, Xu Z, Smyth HDC, Mulder T, *et al*. Physical characterization of component particles included in dry powder inhalers. I. Strategy review and static characteristics. J Pharm Sci. 2007;96(5):1282–301.
48. Hickey AJ, Mansour HM, Telko MJ, Xu Z, Smyth HDC, Mulder T, *et al*. Physical characterization of component particles included in dry powder inhalers. II. Dynamic characteristics. J Pharm Sci. 2007;96(5):1302–19.
49. Hickey AJ, Mansour HM. Delivery of drugs by the pulmonary route. In: Florence AT, Siepmann J, editors. Modern pharmaceutics. New York: Taylor and Francis; 2009. p. 191–219.
50. Edwards DA. The macrotransport of aerosol particles in the lung: aerosol deposition phenomena. J Aerosol Sci. 1995;26(2):293–317.
51. Suarez S, Hickey AJ. Drug properties affecting aerosol behavior. Respir Care. 2000;45(6):652–66.